Biochem. J. (2014) **464**, 85–98 (Printed in Great Britain) doi:10.1042/BJ20131609

Specific aromatic foldamers potently inhibit spontaneous and seeded Aβ42 and Aβ43 fibril assembly

Katelyn M. Seither*, Heather A. McMahon*, Nikita Singh*, Hejia Wang*, Mimi Cushman-Nick*†‡, Geronda L. Montalvo*§, William F. DeGrado‡ and James Shorter*†§[1]

*Department of Biochemistry and Biophysics, Perelman School of Medicine at the University of Pennsylvania, 805b Stellar-Chance Laboratories, 422 Curie Boulevard, Philadelphia, PA 19104, U.S.A.

†Neuroscience Graduate Group, Perelman School of Medicine at the University of Pennsylvania, 805b Stellar-Chance Laboratories, 422 Curie Boulevard, Philadelphia, PA 19104, U.S.A.

‡Department of Pharmaceutical Chemistry, University of California, San Francisco, CVRI-MC Box 3122, San Francisco, CA 94158-9001 U.S.A.

§Biochemistry and Molecular Biophysics Graduate Group, Perelman School of Medicine at the University of Pennsylvania, 805b Stellar-Chance Laboratories, 422 Curie Boulevard, Philadelphia, PA 19104, U.S.A.

Amyloid fibrils are self-propagating entities that spread pathology in several devastating disorders including Alzheimer's disease (AD). In AD, amyloid-β (Aβ) peptides form extracellular plaques that contribute to cognitive decline. One potential therapeutic strategy is to develop inhibitors that prevent Aβ misfolding into proteotoxic conformers. Here, we design specific aromatic foldamers, synthetic polymers with an aromatic salicylamide (Sal) or 3-amino benzoic acid (Benz) backbone, short length (four repetitive units), basic arginine (Arg), lysine (Lys) or citrulline (Cit) side chains, and various N- and C-terminal groups that prevent spontaneous and seeded Aβ fibrillization. Ac-Sal-(Lys-Sal)$_3$-CONH$_2$ and Sal-(Lys-Sal)$_3$-CONH$_2$ selectively inhibited Aβ42 fibrillization, but were ineffective against Aβ43, an overlooked species that is highly neurotoxic and frequently deposited in AD brains. By contrast, (Arg-Benz)$_4$-CONH$_2$ and (Arg-Sal)$_3$-(Cit-Sal)-CONH$_2$ prevented spontaneous and seeded Aβ42 and Aβ43 fibrillization. Importantly, (Arg-Sal)$_3$-(Cit-Sal)-CONH$_2$ inhibited formation of toxic Aβ42 and Aβ43 oligomers and proteotoxicity. None of these foldamers inhibited Sup35 prionogenesis, but Sal-(Lys-Sal)$_3$-CONH$_2$ delayed aggregation of fused in sarcoma (FUS), an RNA-binding protein with a prion-like domain connected with amyotrophic lateral sclerosis and frontotemporal dementia. We establish that inhibitors of Aβ42 fibrillization do not necessarily inhibit Aβ43 fibrillization. Moreover, (Arg-Sal)$_3$-(Cit-Sal)-CONH$_2$ inhibits formation of toxic Aβ conformers and seeding activity, properties that could have therapeutic utility.

Key words: Alzheimer's disease, amyloid, Aβ42 (amyloid-β 42), Aβ43 (amyloid-β 43), foldamer, protein misfolding.

INTRODUCTION

Protein misfolding can be fatal [1,2]. Proteins misfold from soluble species into highly stable, cross-β amyloid fibrils in Alzheimer's disease (AD) and several other neurodegenerative diseases [1,2]. One strategy to combat these disorders is to develop small molecules that inhibit amyloidogenesis and prevent toxic protein misfolding [3–6]. Although daunting challenges face potential small molecule inhibitors of amyloidogenesis [7], they are beginning to reach the clinic. Indeed, tafamidis, a small molecule inhibitor of transthyretin amyloidogenesis treats familial amyloid polyneuropathy, a rare but deadly disease [8,9].

Here, we focus on amyloid-β (Aβ) peptides, Aβ42 and Aβ43, which form amyloid fibrils and accumulate in extracellular plaques that are a hallmark of AD [10–16]. AD is a progressive neurodegenerative disease and the most common cause of dementia worldwide [12]. Aging is a significant risk factor for AD and there are no effective therapies [11]. In Aβ biogenesis, the full-length transmembrane amyloid precursor protein (APP) undergoes sequential cleavage by β- and γ-secretase, resulting in peptides that are 38–43 amino acids in length [10,12]. Aβ42 and Aβ40 are most commonly associated with AD pathology [10–12]. Aβ40 is a more benign, perhaps even neuroprotective species [17,18], which slowly assembles into amyloid fibrils. By contrast, Aβ42 oligomerizes and fibrillizes more rapidly due to two additional C-terminal residues that introduce additional steric zipper hexapeptides that drive assembly [19–21].

Although Aβ peptides longer than Aβ42 are found in AD, they are not a major species and their pathogenic role has been ignored. Recently, this view has changed. Aβ43 is a potent contributor to neurotoxicity in AD [13–15]. Aβ43 contains an additional threonine residue at the C-terminal end and fibrillizes more rapidly than Aβ42 [13]. Aβ43 is more abundant in insoluble fractions than Aβ40 in AD and its presence in senile plaques is directly correlated with cognitive decline [13–16]. Specific inhibitors of Aβ43 misfolding have not been identified and it is unclear whether inhibitors of Aβ42 misfolding will also inhibit Aβ43 misfolding.

Aβ monomers form amyloid via nucleated conformational conversion [22]. First, a subpopulation of Aβ monomers forms molten oligomers, which gradually rearrange into amyloidogenic oligomers that nucleate cross-β fibrils [22,23]. Rearrangement is rate limiting and causes the lag phase of spontaneous fibrillization [22]. During lag phase, Aβ forms diverse oligomeric species, which can be highly toxic [21,24–27]. Upon nucleation, fibrils

Abbreviations: AD, Alzheimer's disease; Aβ, amyloid-β; Benz, 3-amino benzoic acid; DCM, dichloromethane; DIEA, di-isopropylethylamine; DMEM, Dulbecco's modified Eagle's medium; DMF, dimethylformamide; EGCG, (−)-epigallocatechin-3-gallate; HFIP, 1,1,1,3,3,3-hexafluoro-2-propanol; LDH, lactate dehydrogenase; MeOH, methanol; NM, N-terminal and middle domains of Sup35; Sal, salicylamide; TEV, tobbaco etch virus; ThT, thioflavin-T.

[1] To whom correspondence should be addressed (email jshorter@mail.med.upenn.edu).

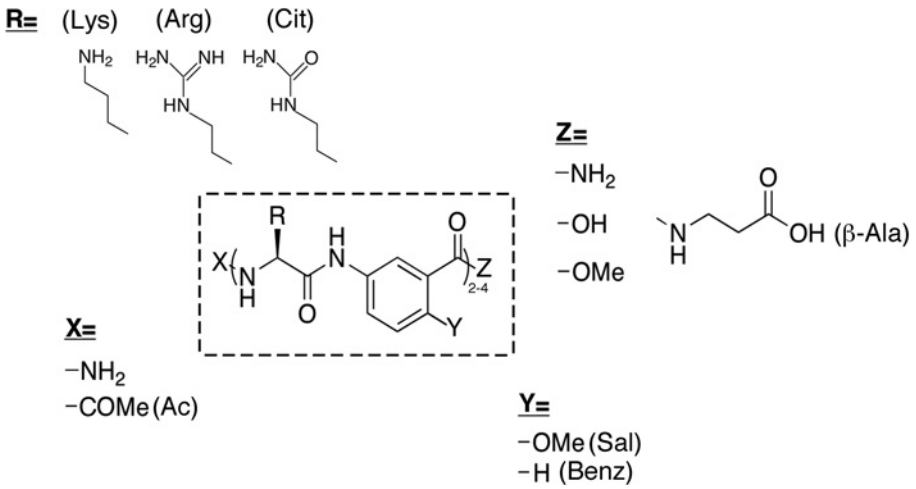

Figure 1 Overview of aromatic foldamer structure

The core foldamer structure is shown in the dashed box, which can be decorated with different moieties at X-, R-, Y- and Z-positions indicated on the periphery. Foldamers possess an aromatic Sal or Benz backbone (Y = OMe or H), Arg, Lys or Cit side chains (R = Arg, Lys or Cit), short length (two to four repetitive units) and various N- (X = NH_2 or Ac) and C- (Z = NH_2, OH, OMe or β-Ala) terminal groups.

rapidly grow via their self-templating ends, which convert Aβ conformers into the cross-β conformation [20,28]. When coupled to fibril fragmentation, this 'seeding' activity enables Aβ fibrils to become self-propagating agents that transmit pathology and disease [1,29–31]. Aβ fibrils also provide catalytic surfaces for 'secondary' nucleation events distinct from fibril elongation [32–34]. Here, lateral Aβ fibril surfaces convert Aβ monomers into toxic oligomers [32–34]. Thus, formation of toxic oligomers and fibrils is intimately linked [32–34]. These secondary nucleation events also help explain Aβ assembly kinetics [32–34]. Aβ forms different cross-β fibril structures termed 'strains', which can differ in toxicity and cause distinct brain pathology [35–38]. Aβ fibrils are usually less toxic than pre-amyloid oligomers [21,39]. However, Aβ fibrils also display toxicity [6,35,36,39]. A key challenge is to manipulate Aβ assembly in a manner that depopulates toxic conformers [7]. Agents that inhibit seeded assembly hold promise for preventing the spread of Aβ pathology in AD.

Numerous potential inhibitors of Aβ misfolding have been explored, including small molecules, peptides, molecular chaperones, protein disaggregases and antibodies [3,6,39–45]. In the present study, we explore a different strategy by pursuing foldamers; non-biological discrete chain molecules that lack a canonical peptide backbone but can fold into specific structures [46]. Foldamers have been utilized as antimicrobial agents and molecular scaffolds [47–50]. Peptides containing non-natural amino acids, similar to foldamers, have been useful for understanding the misfolding of various amyloidogenic peptides [42,51–53]. Foldamers have several advantageous properties that could make them a valuable class of amyloid inhibitors. Due to their semi-rigid backbone, foldamers can assume an organized conformation at low entropic cost with relatively few monomeric units [50,54]. Compared with α peptides, foldamers have greater thermodynamic stability and resist proteases. Furthermore, foldamers of varying lengths with diverse side chains and 3D shapes can be synthesized. These features enable foldamer design for interaction with diverse biological targets [47–50,55]. In the present study, we explore aromatic foldamers as antagonists of Aβ42 and Aβ43 amyloidogenesis.

MATERIALS AND METHODS

Generation of soluble and fibrillar Aβ42 and Aβ43

To produce monomeric Aβ, synthetic lyophilized Aβ42 or Aβ43 (W.M. Keck Facility, Yale University) was dissolved in 1,1,1,3,3,3-hexafluoro-2-propanol (HFIP, Sigma) at 2 mg/ml. HFIP was removed by drying in a speed vacuum for 30 min. The resulting peptide film was dissolved in DMSO to 1 mM. Aβ42 or Aβ43 fibrils for seeding experiments were prepared by diluting monomerized Aβ42 or Aβ43 in KHMD (150 mM KCl, 40 mM Hepes–KOH pH 7.4, 20 mM $MgCl_2$ and 1 mM DTT) to 10 μM. This solution was incubated at 37 °C for 3–5 days with agitation (700 r.p.m.) in an Eppendorf Thermomixer. For seeding experiments, preformed fibrils were briefly sonicated or vortex-mixed prior to use. We also prepared Aβ42 or Aβ43 using a protocol that avoids DMSO. Thus, Aβ42 or Aβ43 was dissolved in HFIP followed by evaporation of the solvent to dryness [56]. Dry peptide films were dissolved in a minimal volume of 60 mM NaOH followed by dilution with deionized water and sonication for 1 min using a bath sonicator. Peptides were diluted to 0.2 mM by adding an equal volume of 20 mM sodium phosphate buffer (PB, Sigma), pH 8 plus 0.2 mM EDTA (PBE). Samples were centrifuged at 16 000 ***g*** for 3 min and subjected to Superdex 75 gel filtration in PBE to remove residual solvent.

Foldamers

Foldamers (Lys-Sal)$_4$-$CONH_2$, (Arg-Benz)$_4$-$CONH_2$, (Lys-Sal)$_4$-COMe, (Lys-Sal)$_4$-COOH, (Lys-Sal)$_4$-COβAla, Ac-(Lys-Sal)$_3$-$CONH_2$, Sal-(Lys-Sal)$_3$-$CONH_2$ and Ac-Sal-(Lys-Sal)$_3$-$CONH_2$ (where Sal is salicylamide and Benz is 3-amino benzoic acid) were from PolyMedix and were dissolved in TBS (50 mM Tris/HCl pH 7.4, 150 mM NaCl) to obtain concentrated stock solutions. Foldamers (Cit-Sal)$_4$-$CONH_2$, (Arg-Sal)$_2$-(Cit-Sal)-(Arg-Sal)-$CONH_2$, (Arg-Sal)$_3$-(Cit-Sal)-$CONH_2$, (Cit-Sal)$_2$-(Arg-Sal)-(Cit-Sal)-$CONH_2$, (Cit-Sal)-(Arg-Sal)-(Cit-Sal)$_2$-$CONH_2$ and (Arg-Sal-Cit-Sal)$_2$-$CONH_2$ were also from PolyMedix. These foldamers were dissolved in 1:1 TBS/DMSO to obtain

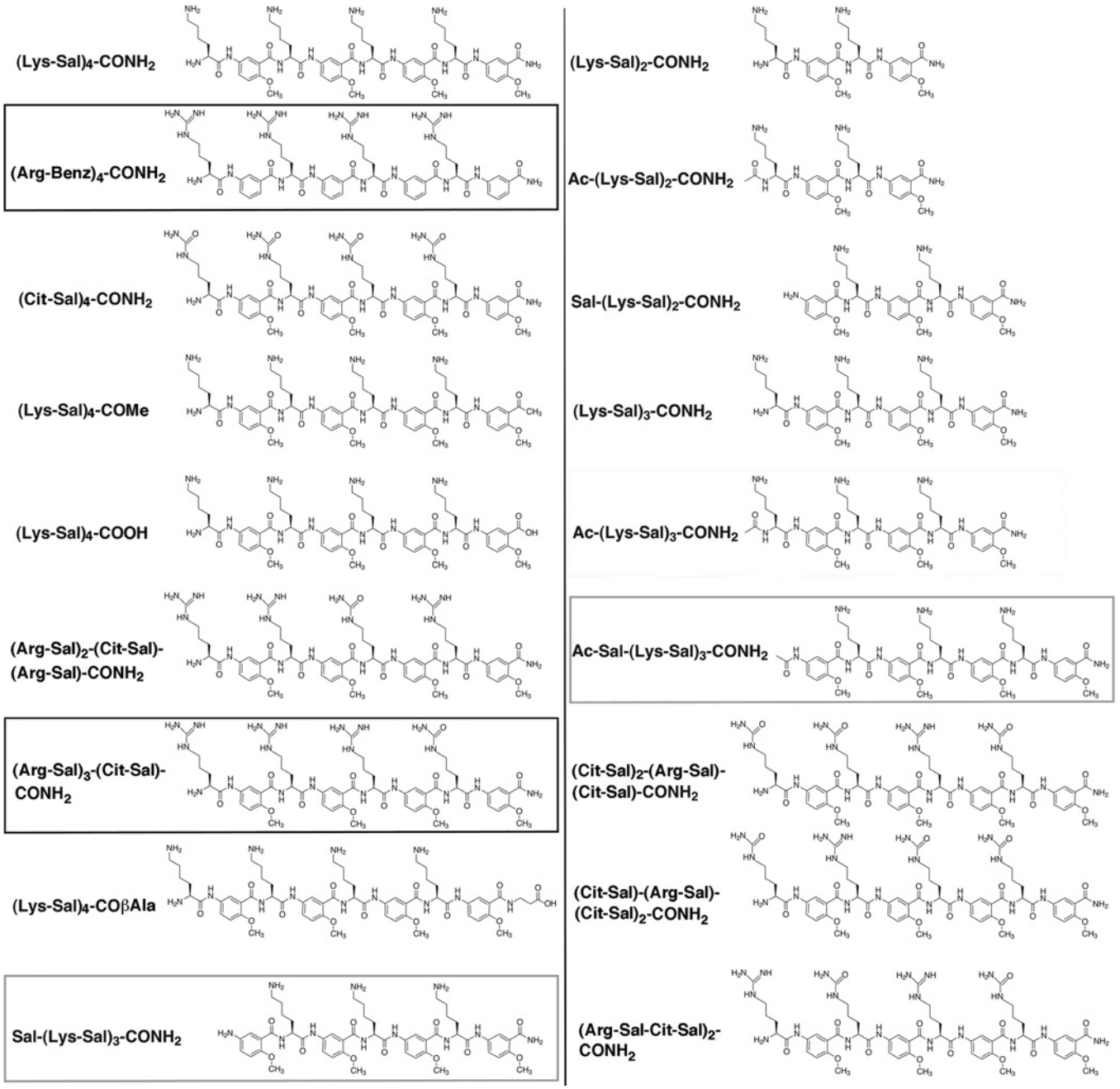

Figure 2 Nomenclature and structure of aromatic foldamers

Three-letter amino acid nomenclature is used to indicate the side chain (Lys, Arg or Cit) and the Sal or Benz backbone is indicated. N- (Ac) and C- (NH_2, OH, OMe or β-Ala) terminal groups are also indicated. Foldamers that inhibit spontaneous Aβ42 and Aβ43 fibrillization, $(Arg\text{-}Benz)_4\text{-}CONH_2$ and $(Arg\text{-}Sal)_3\text{-}(Cit\text{-}Sal)\text{-}CONH_2$, are boxed in black. Foldamers that inhibit spontaneous Aβ42 fibrillization but not spontaneous Aβ43 fibrillization, $Sal\text{-}(Lys\text{-}Sal)_3\text{-}CONH_2$ and $Ac\text{-}Sal\text{-}(Lys\text{-}Sal)_3\text{-}CONH_2$, are boxed in grey.

concentrated stocks. Subsequent dilutions were made from these stocks to appropriate concentrations in KHMD or PBE.

Foldamers $(Lys\text{-}Sal)_2\text{-}CONH_2$, $Ac\text{-}(Lys\text{-}Sal)_2\text{-}CONH_2$, $Sal\text{-}(Lys\text{-}Sal)_2\text{-}CONH_2$, $(Lys\text{-}Sal)_3\text{-}CONH_2$ and $Ac\text{-}(Lys\text{-}Sal)_3\text{-}CONH_2$ were synthesized at room temperature on a 100 μmol scale using rink amide resin (GemScript Corporation, 0.6 mmol/g substitution) for support of alternating α- (Bachem) and aromatic amino acids. Resin was swelled in 100 % dimethylformamide (DMF, Fisher Scientific) for 1 h, followed by a 30 min deprotection using 5 % piperazine (Sigma–Aldrich) in DMF. The first residue was coupled to the resin using 3 equiv. of amino acid, 2.8 equiv. of 2-(6-chloro-1H-benzotriazole-1-yl)-1,1,3,3-tetramethylaminium hexafluorophosphate (HCTU, GL Biosciences) activator and 7.5 equiv. of di-isopropylethylamine (DIEA, CHEM-IMPEX International), shaking for 1 h at room temperature. The resin was washed three times each with DMF, dichloromethane (DCM, Fisher Scientific) and DMF. This step was followed by deprotection (as above). Coupling and deprotection steps were cycled for the remaining residues in each respective peptide sequence. After deprotection of the

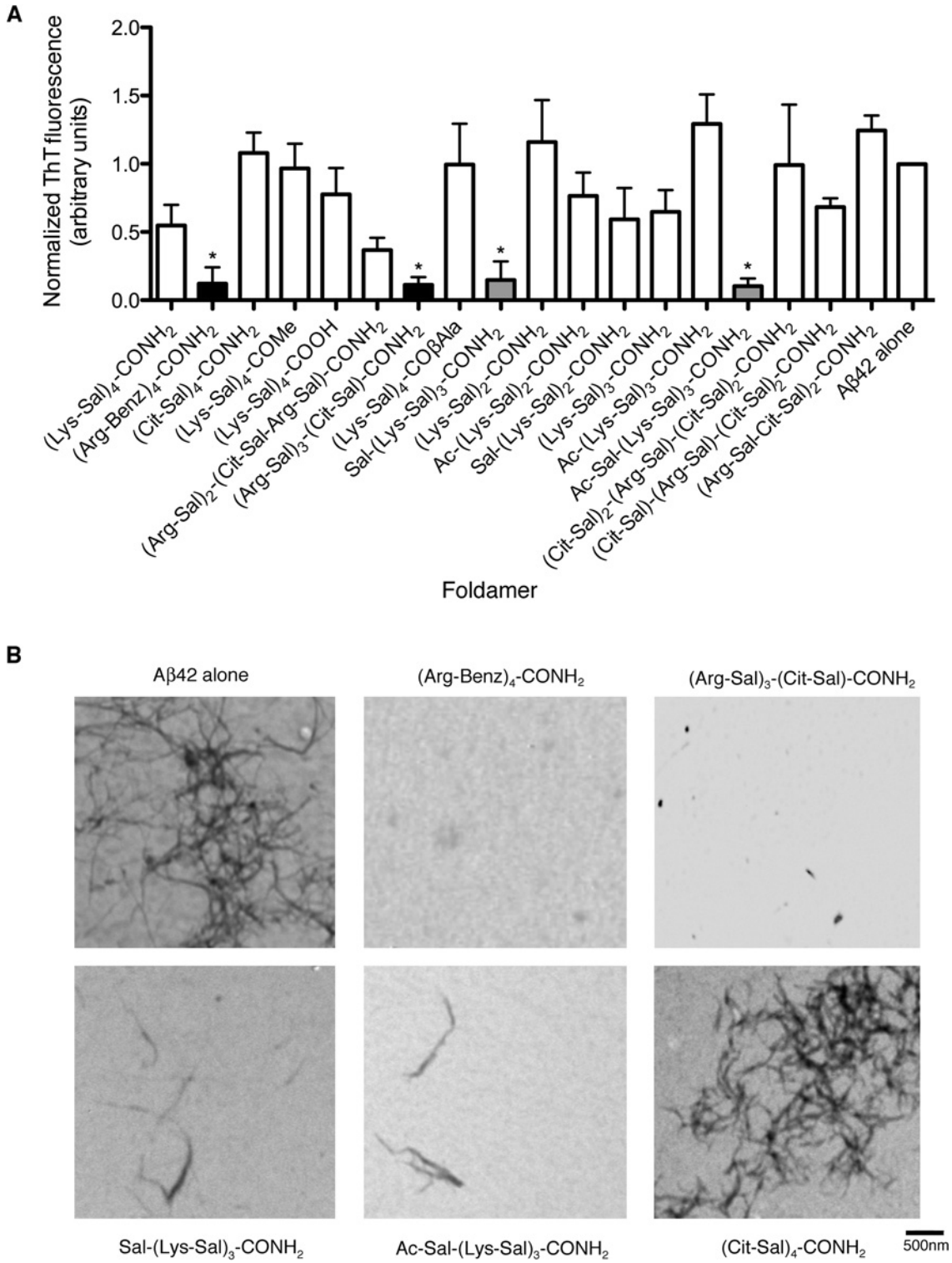

Figure 3 (Arg-Benz)$_4$-CONH$_2$, (Arg-Sal)$_3$-(Cit-Sal)-CONH$_2$, Sal-(Lys-Sal)$_3$-CONH$_2$ and Ac-Sal-(Lys-Sal)$_3$-CONH$_2$ inhibit spontaneous Aβ42 fibrillization

(**A**) Aβ42 (5 μM) was incubated with agitation for 8 h at 25 °C plus or minus the indicated foldamer (10 μM). Aβ42 fibrillization was assessed by ThT fluorescence. Values represent means $\pm$ S.E.M. ($n = 3$–6). A one-way ANOVA with the post-hoc Dunnett's multiple comparisons test was used to compare Aβ42 alone to each Aβ42 plus foldamer condition (* denotes $P < 0.05$). Foldamers that selectively inhibit Aβ42 fibrillization are indicated by grey bars and foldamers that inhibit Aβ42 and Aβ43 fibrillization are indicated by black bars. (**B**) Aβ42 (5 μM) was incubated with agitation for 4 h at 25 °C in the absence or presence of the indicated foldamer (10 μM). Aβ42 fibrillization was assessed by EM. Scale bar, 500 nm.

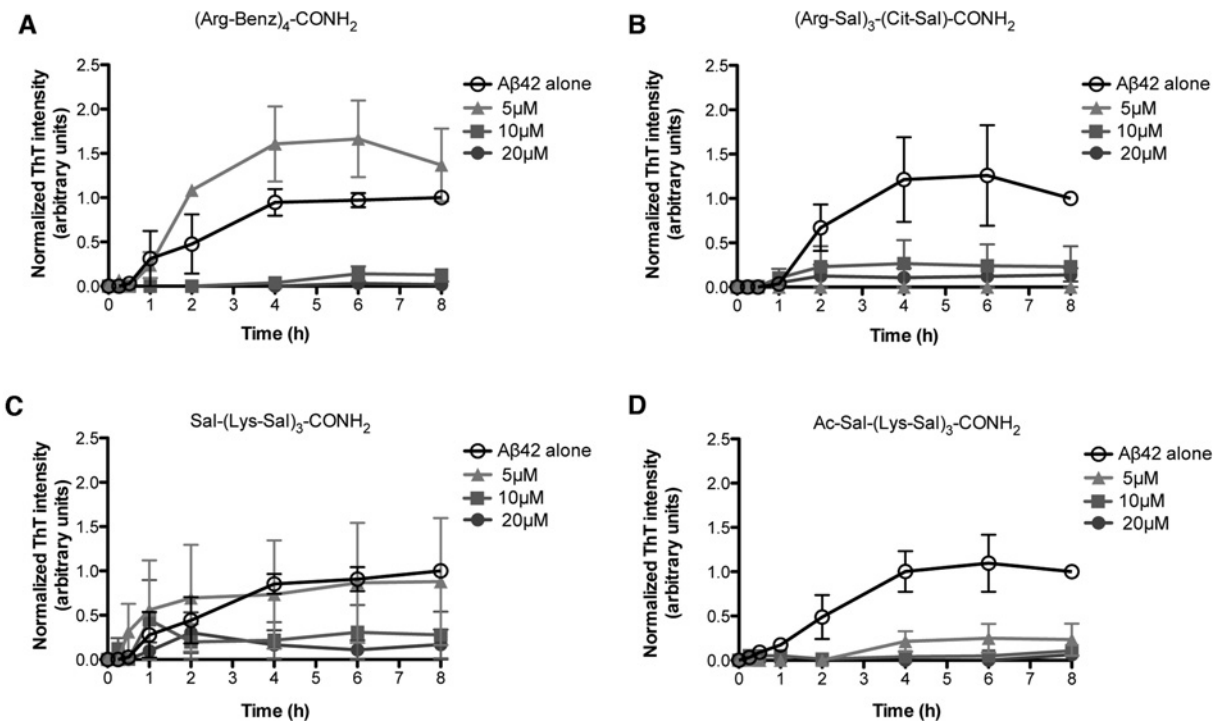

Figure 4 Effect of inhibitory foldamers on spontaneous Aβ42 fibrillization kinetics

(**A**–**D**) Aβ42 (5 μM) was incubated with agitation for 0–8 h at 25 °C in the absence (open circles) or presence of 5 μM (filled triangles), 10 μM (filled squares) or 20 μM (filled circles) $(Arg\text{-}Benz)_4\text{-}CONH_2$ (**A**), $(Arg\text{-}Sal)_3\text{-}(Cit\text{-}Sal)\text{-}CONH_2$ (**B**), $Sal\text{-}(Lys\text{-}Sal)_3\text{-}CONH_2$ (**C**) or $Ac\text{-}Sal\text{-}(Lys\text{-}Sal)_3\text{-}CONH_2$ (**D**). Aβ42 fibrillization was assessed by ThT fluorescence. Values represent means ± S.E.M. ($n = 3$).

final residue the product was rinsed [three times with DMF, three times with DCM, three times with DMF and three times with methanol (MeOH)] and dried with MeOH. This product was split in half. The first half was re-swelled in DMF and acetylated by incubating the resin in 5 % acetic anhydride in 2.5 % DIEA and 92.5 % DMF for 10 min. This acetylated portion was rinsed and dried (as above). Next, both halves (one with a N-terminal acetyl and a second with a N-terminal free amide) were cleaved from the resin using a cocktail of 2:2:2:94 H_2O/TIS (tri-isopropyl silane)/anisole/TFA (trifluoroacetic acid; Sigma–Aldrich) for 2 h at room temperature. The peptide solution was filtered from the resin and precipitated using 1:1 cold ethyl ether:hexane. The precipitate was dried by lyophilization. The mass and purity of each product was verified by MALDI–TOF MS (Brucker microflex LRF) and analytical HPLC (C18 column). Dried crude foldamer was purified by preparative reverse-phase HPLC, dried by lyophilization and mass and purity was verified as above. All samples were prepared by directly dissolving lyophilized foldamer into TBS buffer to 2 mM.

Spontaneous and seeded Aβ42, Aβ43 and N-terminal and middle domain of Sup35 (NM) fibrillization

For spontaneous fibrillization, soluble Aβ42 or Aβ43 (1 mM) in DMSO was diluted to 5 μM in KHMD containing 25 μM thioflavin-T (ThT) plus or minus foldamer (0–20 μM). For seeded fibrillization, preformed Aβ42 or Aβ43 fibrils (10 μM monomer) were added at a final concentration of 0.1 μM (monomer). Alternatively, Aβ42 or Aβ43 were prepared using just HFIP and were assembled at 5 μM in PBE containing 25 μM ThT plus or minus foldamer (20 μM). NM was purified as described [57]. NM (5 μM) was assembled in KHMD containing 25 μM ThT plus or minus foldamer (20 μM). For seeded fibrillization, preformed NM fibrils (5 μM monomer) were added at a final concentration of 0.1 μM (monomer). Reactions were conducted in 96-well plates and incubated at 25 °C in a TECAN Safire II plate reader (Tecan USA) for up to 8 h with agitation. ThT fluorescence was measured at the indicated times. The excitation wavelength was 450 nm (5 nm bandwidth) and the emission wavelength was 482 nm (10 nm bandwidth). ThT fluorescence values reported are arbitrary and are normalized to the final assembly time point of the Aβ alone condition.

FUS aggregation

GST–TEV–FUS was purified as described [58]. Aggregation was initiated by addition of tobbaco etch virus (TEV) protease to GST–TEV–FUS (5 μM) plus or minus foldamer (20 μM) in assembly buffer (50 mM Tris/HCl pH 8, 0.2 M trehalose and 20 mM glutathione). Aggregation was for 0–90 min at 25 °C without agitation in a 96-well plate and was assessed by turbidity (absorbance at 395 nm) using a Tecan Infinite M1000 plate reader [58]. No aggregation occurred unless TEV protease was added to separate GST from FUS [58]. SDS/PAGE and Coomassie staining revealed that foldamers did not inhibit cleavage of GST–TEV–FUS by TEV.

Electron microscopy

Reactions were adhered on to 300-mesh-formvar carbon-coated EM grids overnight before being negatively stained with 2 % uranyl acetate for 2 min and rinsed with milli-Q distilled water. Micrographs were acquired using a JEOL 1010 TEM (Jeol USA).

Tracking A11-reactive Aβ42 or Aβ43 conformers

The oligomer-specific A11 antibody was used to detect toxic Aβ42 or Aβ43 oligomers by ELISA as described [21]. Foldamers did not cross-react with A11.

Toxicity assays

SH-SY5Y human neuroblastoma cells were maintained in Dulbecco's modified Eagle's medium (DMEM) plus 10 mM Hepes, 10 % FBS, 4 mM glutamine, penicillin (200 units/ml) and streptomycin (200 μg/ml) in 5 % CO_2 at 37 °C. Cells were differentiated in serum-free DMEM with N2 supplement and 10 μM all-*trans*-retinoic acid before use. Cells were plated at (10000 cells/well) in 96-well plates and grown overnight. Medium was removed and Aβ conformers or controls were added and cells were incubated for 24 h at 37 °C. Toxicity was assessed using an MTT kit (Tox-1; Sigma) or via lactate dehydrogenase (LDH) release using the CytoTox-ONE™ kit (Promega). Toxicity values were normalized to the buffer control without Aβ.

RESULTS AND DISCUSSION

Rationale and foldamer design

As potential inhibitors of Aβ42 and Aβ43 amyloidogenesis, we explored aromatic foldamers (Figures 1 and 2). Some of these foldamers were originally synthesized as inhibitors of heparin and are rich in aromatic and positively charged groups [55]. They possess an aromatic salicylamide (Sal) or 3-amino benzoic acid (Benz) backbone (Figure 1; Y = OMe or H), lysine (Lys), arginine (Arg) or citrulline (Cit) side chains (Figure 1; R = Lys, Arg or Cit), short length (two to four repetitive units) (Figure 1) and various N- (Figure 1; X = NH_2 or COMe [Ac]) and C- (Figure 1; Z = NH_2, OH, OMe or β-Ala) terminal groups. We selected this design for four reasons. First, the aromatic backbone is similar to ones employed by Nowick et al. [42,51–53] in protein aggregation inhibitors. Secondly, interactions between aromatic residues within short amyloidogenic peptides mediate molecular recognition during fibrillization [59]. Moreover, polyphenols such as (−)-epigallocatechin-3-gallate (EGCG) inhibit amyloidogenesis and prevent cytotoxicity [57,59–61]. Thus, the aromatic foldamer spine might antagonize aromatic interactions critical for fibrillization. Thirdly, the aromatic foldamers investigated are approximately the same length (two to four repetitive units) as steric zipper hexapeptides that form amyloid [19]. Finally, basic side chains, particularly arginine exert hydrotropic effects and prevent protein aggregation [62].

Foldamer inhibition screen

We tested 18 aromatic foldamers (Figure 2) for inhibition of spontaneous (i.e. in the absence of preformed fibrils) Aβ42 fibrillization. The majority of foldamers did not significantly inhibit Aβ42 fibrillization (Figure 3A). However, $(Arg\text{-}Benz)_4\text{-}CONH_2$, $(Arg\text{-}Sal)_3\text{-}(Cit\text{-}Sal)\text{-}CONH_2$, $Sal\text{-}(Lys\text{-}Sal)_3\text{-}CONH_2$ and $Ac\text{-}Sal\text{-}(Lys\text{-}Sal)_3\text{-}CONH_2$ were strong inhibitors (Figure 2 boxed in black or grey; Figures 3A and 3B; Figures 4A–4D). $(Arg\text{-}Sal)_3\text{-}(Cit\text{-}Sal)\text{-}CONH_2$ was the most potent with an IC_{50} of ~1.6 μM.

Several important foldamer properties emerge for inhibition of Aβ42 fibrillization. First, a foldamer must have a backbone with at least four aromatic units to antagonize Aβ42 fibrillization. Thus, $(Lys\text{-}Sal)_2\text{-}CONH_2$, $Ac\text{-}(Lys\text{-}Sal)_2\text{-}CONH_2$, $Sal\text{-}(Lys\text{-}Sal)_2\text{-}CONH_2$, $(Lys\text{-}Sal)_3\text{-}CONH_2$ and $Ac\text{-}(Lys\text{-}Sal)_3\text{-}CONH_2$ failed to inhibit assembly (Figures 2 and 3A). Secondly, foldamers with more than three lysine or citrulline side chains were ineffective, encompassing: $(Lys\text{-}Sal)_4\text{-}CONH_2$, $(Cit\text{-}Sal)_4\text{-}CONH_2$, $(Lys\text{-}Sal)_4\text{-}COMe$, $(Lys\text{-}Sal)_4\text{-}COOH$ and $(Lys\text{-}Sal)_4\text{-}CO\beta Ala$ (Figures 2 and 3A). By contrast, $Sal\text{-}(Lys\text{-}Sal)_3\text{-}CONH_2$ and $Ac\text{-}Sal\text{-}(Lys\text{-}Sal)_3\text{-}CONH_2$, which possess three lysine side chains and four aromatic backbone units, were potent inhibitors (Figures 2 and 3A). Thirdly, foldamers with three or more consecutive Arg side chains were effective inhibitors. Thus, $(Arg\text{-}Benz)_4\text{-}CONH_2$ and $(Arg\text{-}Sal)_3\text{-}(Cit\text{-}Sal)\text{-}CONH_2$ were potent inhibitors, whereas $(Arg\text{-}Sal)_2\text{-}(Cit\text{-}Sal)\text{-}(Arg\text{-}Sal)\text{-}CONH_2$, $(Cit\text{-}Sal)_2\text{-}(Arg\text{-}Sal)\text{-}(Cit\text{-}Sal)\text{-}CONH_2$, $(Cit\text{-}Sal)\text{-}(Arg\text{-}Sal)\text{-}(Cit\text{-}Sal)_2\text{-}CONH_2$ and $(Arg\text{-}Sal\text{-}Cit\text{-}Sal)_2\text{-}CONH_2$ were ineffective (Figures 2 and 3A).

Select small molecules that inhibit Aβ42 fibrillization also disassemble Aβ42 fibrils [4,57,60]. However, even when present in 4-fold molar excess, $(Arg\text{-}Benz)_4\text{-}CONH_2$, $(Arg\text{-}Sal)_3\text{-}(Cit\text{-}Sal)\text{-}CONH_2$, $Sal\text{-}(Lys\text{-}Sal)_3\text{-}CONH_2$ and $Ac\text{-}Sal\text{-}(Lys\text{-}Sal)_3\text{-}CONH_2$ did not disassemble Aβ42 fibrils after 24 h (results not shown). Thus, these foldamers do not reverse Aβ42 fibrillization.

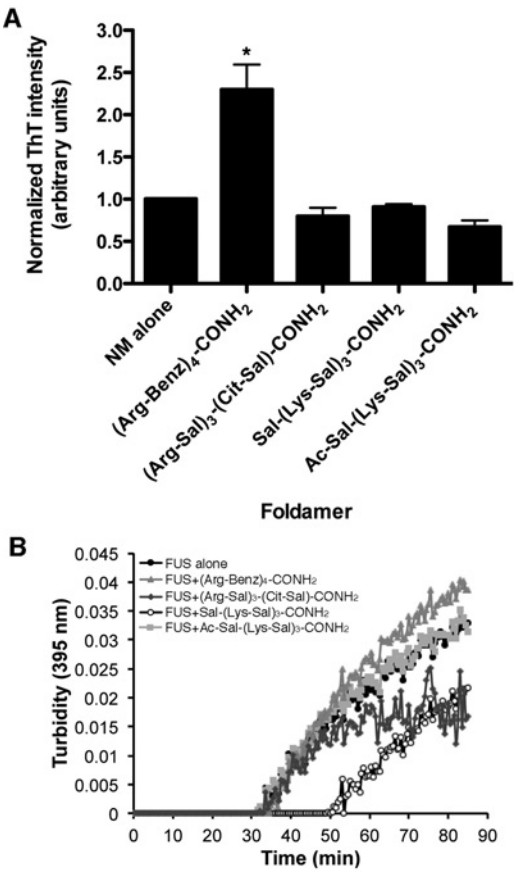

Figure 5 Sal-(Lys-Sal)$_3$-CONH$_2$ has no effect on NM fibrillization but delays FUS aggregation

(**A**) NM (5 μM) was incubated with agitation for 4 h at 25 °C plus or minus the indicated foldamer (20 μM). NM fibrillization was assessed by ThT fluorescence. Values represent means ± S.E.M. (n = 3). A one-way ANOVA with the *post-hoc* Dunnett's multiple comparisons test was used to compare NM alone to each NM plus foldamer condition (* denotes $P < 0.05$). (**B**) GST-FUS (5 μM) was incubated in the presence of the indicated foldamer (20 μM) plus TEV protease at 25 °C for 0–90 min. Turbidity measurements (absorbance at 395 nm) were taken every minute to assess aggregation. A representative dataset is shown.

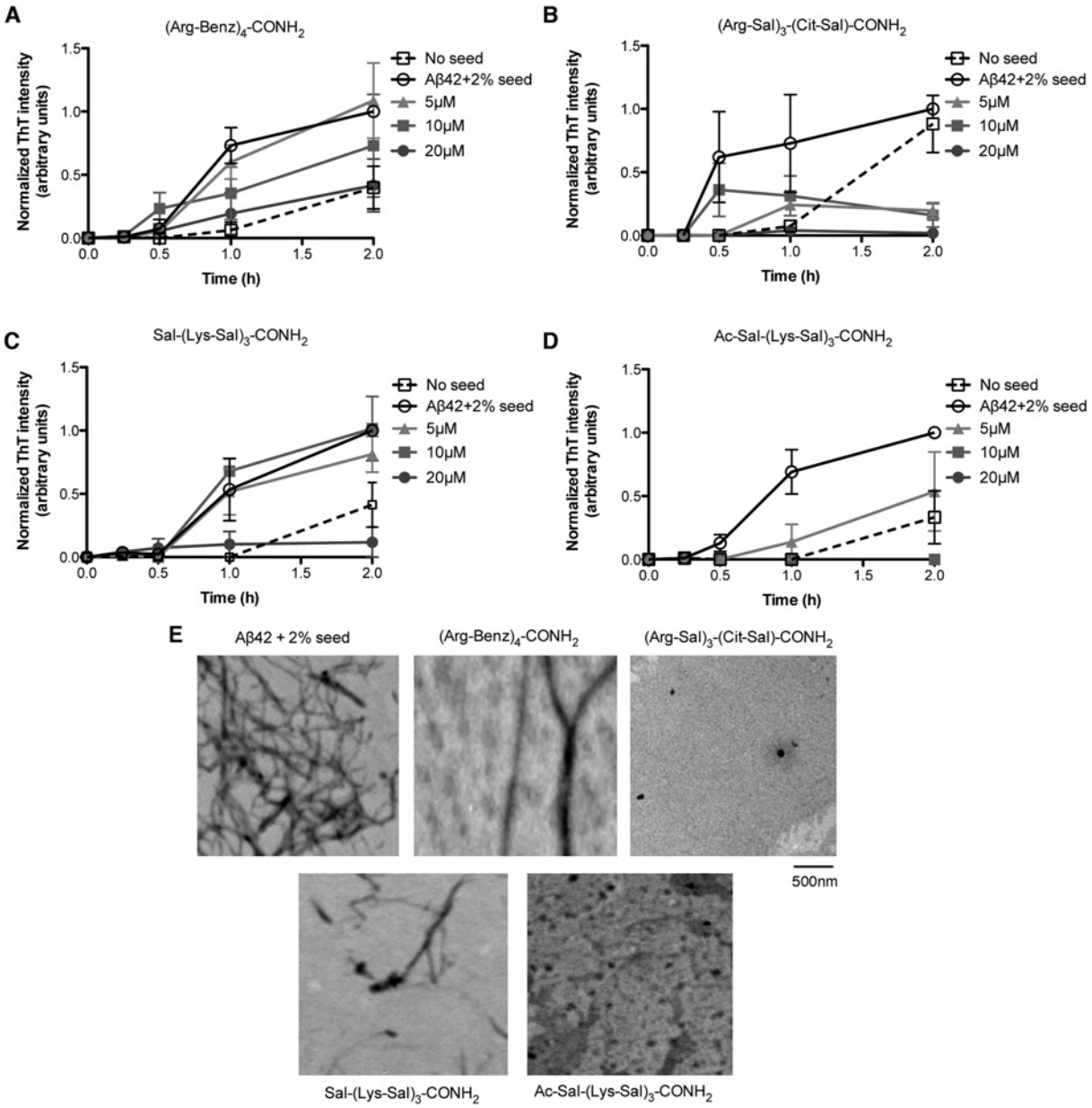

Figure 6 (Arg-Sal)$_3$-(Cit-Sal)-CONH$_2$ and Ac-Sal-(Lys-Sal)$_3$-CONH$_2$ inhibit seeded Aβ42 fibrillization

(**A**–**D**) Aβ42 (5 μM) was incubated with agitation for 0–2 h at 25 °C without (open squares) or with Aβ42 fibril seed (0.1 μM monomer) in the absence (open circles) or presence of 5 μM (filled triangles), 10 μM (filled squares) or 20 μM (filled circles) (Arg-Benz)$_4$-CONH$_2$ (**A**), (Arg-Sal)$_3$-(Cit-Sal)-CONH$_2$ (**B**), Sal-(Lys-Sal)$_3$-CONH$_2$ (**C**) or Ac-Sal-(Lys-Sal)$_3$-CONH$_2$ (**D**). Aβ42 fibrillization was assessed by ThT fluorescence. Values represent means ± S.E.M. ($n = 3$). (**E**) Aβ42 (5 μM) plus Aβ42 fibril seed (0.1 μM monomer) was incubated with agitation for 4 h at 25 °C plus or minus the indicated foldamer (10 μM). Aβ42 fibrillization was assessed by EM. Scale bar, 500 nm.

Foldamers that inhibit Aβ42 fibrillization do not inhibit NM fibrillization

Next, we assessed foldamer specificity by testing whether they inhibited amyloidogenesis of the prion domain, NM, of yeast Sup35 [63]. (Arg-Benz)$_4$-CONH$_2$, (Arg-Sal)$_3$-(Cit-Sal)-CONH$_2$, Sal-(Lys-Sal)$_3$-CONH$_2$ and Ac-Sal-(Lys-Sal)$_3$-CONH$_2$ did not inhibit NM fibrillization (Figure 5A). In the presence of (Arg-Benz)$_4$-CONH$_2$, NM formed fibrils that exhibited greater ThT fluorescence (Figure 5A). EM revealed that purely NM fibrils formed in the presence or absence of (Arg-Benz)$_4$-CONH$_2$ and sedimentation analysis revealed that equal quantities of NM formed fibrils (results not shown). Thus, (Arg-Benz)$_4$-CONH$_2$ does not stimulate NM fibrillization. Rather, we suggest that NM accesses a different prion strain in the presence of (Arg-Benz)$_4$-CONH$_2$. NM accesses different prion strains in the presence of certain small molecules, such as EGCG [57,63]. None of these foldamers inhibited seeded NM fibrillization (results not shown). Thus, these foldamers are not generic inhibitors of amyloidogenesis.

Sal-(Lys-Sal)$_3$-CONH$_2$ delays FUS aggregation

To further test specificity, we assessed inhibition of aggregation of FUS, an RNA-binding protein with a prion-like domain, which is connected with amyotrophic lateral sclerosis and frontotemporal dementia [1,58,64].

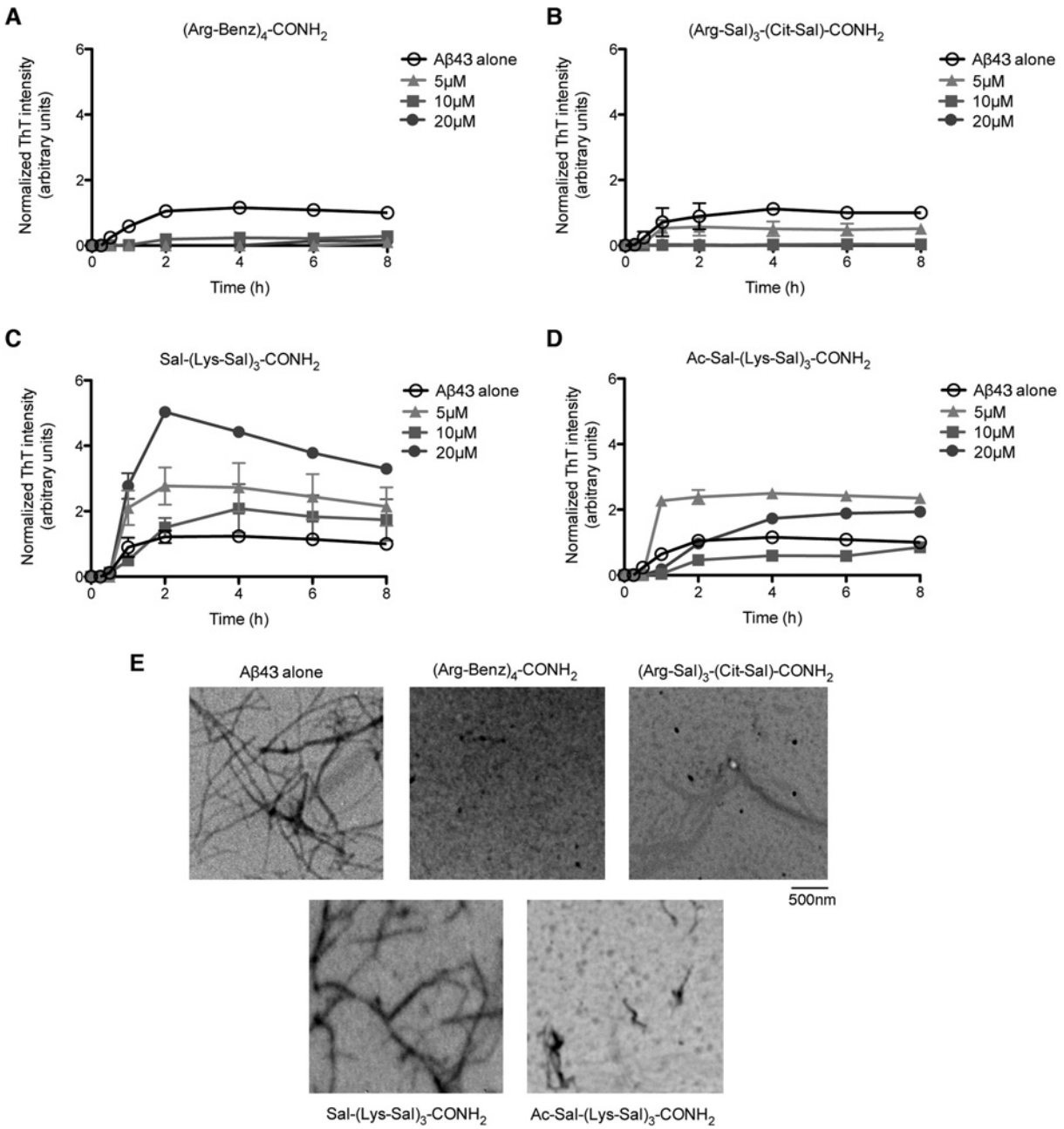

Figure 7 (Arg-Benz)$_4$-CONH$_2$ and (Arg-Sal)$_3$-(Cit-Sal)-CONH$_2$ inhibit spontaneous Aβ43 fibrillization

(**A**–**D**) Aβ43 (5 μM) was incubated with agitation for 0–8 h at 25 °C in the absence (open circles) or presence of 5 μM (filled triangles), 10 μM (filled squares) or 20 μM (filled circles) (Arg-Benz)$_4$-CONH$_2$ (**A**), (Arg-Sal)$_3$-(Cit-Sal)-CONH$_2$ (**B**), Sal-(Lys-Sal)$_3$-CONH$_2$ (**C**) or Ac-Sal-(Lys-Sal)$_3$-CONH$_2$ (**D**). Aβ43 fibrillization was assessed by ThT fluorescence. Values represent means $\pm$ S.E.M. ($n = 3$). (**E**) Aβ43 (5 μM) was incubated with agitation for 4 h at 25 °C in the absence or presence of the indicated foldamer (10 μM). Aβ43 fibrillization was assessed by EM. Scale bar, 500 nm.

(Arg-Benz)$_4$-CONH$_2$, (Arg-Sal)$_3$-(Cit-Sal)-CONH$_2$ and Ac-Sal-(Lys-Sal)$_3$-CONH$_2$ did not inhibit FUS aggregation (Figure 5B). Interestingly, Sal-(Lys-Sal)$_3$-CONH$_2$ delayed FUS aggregation (Figure 5B). Sal-(Lys-Sal)$_3$-CONH$_2$ could serve as a lead foldamer to be optimized against FUS misfolding.

(Arg-Sal)$_3$-(Cit-Sal)-CONH$_2$ and Ac-Sal-(Lys-Sal)$_3$-CONH$_2$ inhibit seeded Aβ42 fibrillization

(Arg-Benz)$_4$-CONH$_2$ and Sal-(Lys-Sal)$_3$-CONH$_2$ only inhibited seeded Aβ42 fibrillization when present at a 4-fold molar excess over Aβ42 (Figures 6A and 6C, filled circles; Figure 6E). Even at this high concentration, some fibrillization occurred in the presence of (Arg-Benz)$_4$-CONH$_2$ (Figure 6A, filled circles) but was very limited by Sal-(Lys-Sal)$_3$-CONH$_2$ (Figure 6C, filled circles). Thus, (Arg-Benz)$_4$-CONH$_2$ and Sal-(Lys-Sal)$_3$-CONH$_2$ are more potent inhibitors of spontaneous Aβ42 fibrillization (Figures 4A and 4C) than seeded Aβ42 fibrillization (Figures 6A and 6C). (Arg-Benz)$_4$-CONH$_2$ and Sal-(Lys-Sal)$_3$-CONH$_2$ likely preferentially inhibit the rearrangement of Aβ42 oligomers into fibril-nucleating species [22]. Once Aβ42 fibrils have formed,

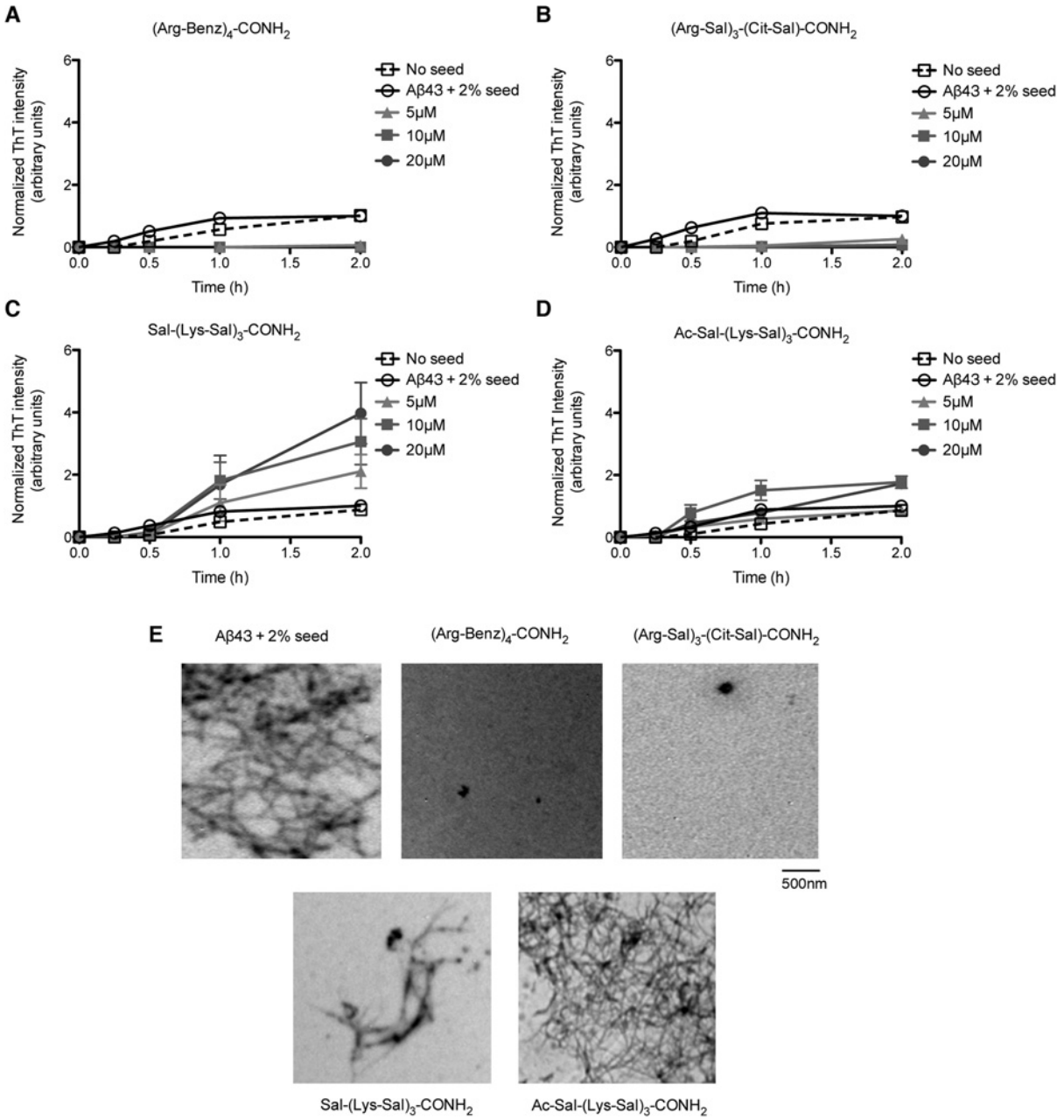

Figure 8 Foldamers (Arg-Benz)$_4$-CONH$_2$ and (Arg-Sal)$_3$-(Cit-Sal)-CONH$_2$ inhibit seeded Aβ43 fibrillization

(**A**–**D**) Aβ43 (5 μM) was incubated with agitation for 0–2 h at 25 °C without (open squares) or with Aβ43 fibril seed (0.1 μM monomer) in the absence (open circles) or presence of 5 μM (filled triangles), 10 μM (filled squares) or 20 μM (filled circles) (Arg-Benz)$_4$-CONH$_2$ (**A**), (Arg-Sal)$_3$-(Cit-Sal)-CONH$_2$ (**B**), Sal-(Lys-Sal)$_3$-CONH$_2$ (**C**) or Ac-Sal-(Lys-Sal)$_3$-CONH$_2$ (**D**). Aβ43 fibrillization was assessed by ThT fluorescence. Values represent means ± S.E.M. ($n = 3$). (**E**) Aβ43 (5 μM) plus Aβ43 fibril seed (0.1 μM monomer) was incubated with agitation for 4 h at 25 °C plus or minus the indicated foldamer (10 μM). Aβ42 fibrillization was assessed by EM. Scale bar, 500 nm.

(Arg-Benz)$_4$-CONH$_2$ and Sal-(Lys-Sal)$_3$-CONH$_2$ have reduced ability to inhibit assembly.

Ac-Sal-(Lys-Sal)$_3$-CONH$_2$ and (Arg-Sal)$_3$-(Cit-Sal)-CONH$_2$ inhibited seeded Aβ42 fibrillization at all concentrations tested (Figures 6B, 6D and 6E). (Arg-Sal)$_3$-(Cit-Sal)-CONH$_2$ was more potent with an IC_{50} of ~2.5 μM (Figures 6B, 6D and 6E). Thus, Ac-Sal-(Lys-Sal)$_3$-CONH$_2$ and (Arg-Sal)$_3$-(Cit-Sal)-CONH$_2$ inhibit Aβ42 fibrillization even after formation of species that nucleate fibrillization.

(Arg-Benz)$_4$-CONH$_2$ and (Arg-Sal)$_3$-(Cit-Sal)-CONH$_2$ inhibit spontaneous Aβ43 fibrillization

It is unknown whether inhibitors that target Aβ42 will also be active against Aβ43. In the absence of foldamer, Aβ43 fibrillization assembled more rapidly than Aβ42 (Figures 4A–4D, and 7A–7D). Sal-(Lys-Sal)$_3$-CONH$_2$ and Ac-Sal-(Lys-Sal)$_3$-CONH$_2$ did not block spontaneous Aβ43 fibrillization (Figures 7C–7E). Indeed, Sal-(Lys-Sal)$_3$-CONH$_2$ enabled Aβ43

fibrils to form that exhibited higher ThT fluorescence (Figures 7C and 7E) and sedimentation analysis revealed that equal quantities of Aβ43 formed fibrils (results not shown). Thus, Sal-(Lys-Sal)$_3$-CONH$_2$ does not stimulate Aβ43 fibrillization. Rather, Aβ43 may access a different amyloid strain in the presence of Sal-(Lys-Sal)$_3$-CONH$_2$. These findings suggest that potent inhibitors of spontaneous Aβ42 fibrillization may not inhibit spontaneous Aβ43 fibrillization. By contrast, (Arg-Benz)$_4$-CONH$_2$ and (Arg-Sal)$_3$-(Cit-Sal)-CONH$_2$ blocked spontaneous Aβ43 fibrillization (Figures 7A, 7B and E). In both cases, small oligomers were the major species (Figure 7E). The IC$_{50}$ of (Arg-Sal)$_3$-(Cit-Sal)-CONH$_2$ was $\sim$3.1 μM (Figures 7A and 7B).

(Arg-Benz)$_4$-CONH$_2$ and (Arg-Sal)$_3$-(Cit-Sal)-CONH$_2$ inhibit seeded Aβ43 fibrillization

Aβ43 fibrils eliminated the lag phase of Aβ43 assembly (Figures 8A–8D, compare open squares and open circles). Sal-(Lys-Sal)$_3$-CONH$_2$ and Ac-Sal-(Lys-Sal)$_3$-CONH$_2$ did not inhibit seeded Aβ43 fibrillization (Figures 8C–8E). Sal-(Lys-Sal)$_3$-CONH$_2$ enabled Aβ43 to access fibrillar forms that generated a higher ThT fluorescence signal, perhaps indicative of a distinct Aβ43 amyloid strain (Figure 8C). By contrast, (Arg-Benz)$_4$-CONH$_2$ and (Arg-Sal)$_3$-(Cit-Sal)-CONH$_2$ blocked seeded Aβ43 fibrillization (Figures 8A, 8B and 8E). The IC$_{50}$ of (Arg-Sal)$_3$-(Cit-Sal)-CONH$_2$ against seeded Aβ43 fibrillization was $\sim$1.7 μM.

Foldamers inhibit Aβ42 and Aβ43 fibrillization under different assembly conditions

Next, we established that foldamers inhibited spontaneous and seeded Aβ42 and Aβ43 fibrillization under different assembly conditions, which might support formation of different amyloid strains. Thus, we avoided DMSO in Aβ preparation and assembled in a higher pH buffer. Under these conditions, a negative control foldamer, (Cit-Sal)$_4$-CONH$_2$, had no effect (Figure 9). By contrast, (Arg-Benz)$_4$-CONH$_2$, (Arg-Sal)$_3$-(Cit-Sal)-CONH$_2$, Sal-(Lys-Sal)$_3$-CONH$_2$ and Ac-Sal-(Lys-Sal)$_3$-CONH$_2$ inhibited spontaneous and seeded Aβ42 fibrillization (Figure 9), whereas only (Arg-Benz)$_4$-CONH$_2$ and (Arg-Sal)$_3$-(Cit-Sal)-CONH$_2$ inhibited spontaneous and seeded Aβ43 fibrillization (Figure 9).

(Arg-Sal)$_3$-(Cit-Sal)-CONH$_2$ antagonizes formation of A11-reactive Aβ42 and Aβ43 oligomers

Could foldamers inhibit the formation of toxic Aβ42 and Aβ43 oligomers? To assess toxic Aβ42 and Aβ43 oligomer formation, we employed the conformation-specific A11 antibody, which specifically recognizes preamyloid oligomers formed by multiple proteins, including Aβ42, but not monomers or fibrils [21]. We assessed formation of A11-reactive species at the start of spontaneous assembly (0 h), at the end of lag phase (0.5 h), and at the endpoint of fibrillization (4 h). In the absence of Aβ42 and Aβ43, no A11 immunoreactivity was observed (results not shown). For Aβ42 and Aβ43, A11-reactive conformers were scarce at the start of the reaction (Figure 10A, buffer controls, black bars), abundant at end of lag phase (Figure 10A, buffer controls, grey bars), and declined once fibrillization was complete (Figure 10A, buffer controls, white bars). Aβ43 exhibited greater A11-immunoreactivity than Aβ42 and appears more prone to accessing this toxic conformation (Figure 10A).

A negative control foldamer, (Cit-Sal)$_4$-CONH$_2$ (Figure 2), had no effect on the appearance and disappearance of A11-reactive

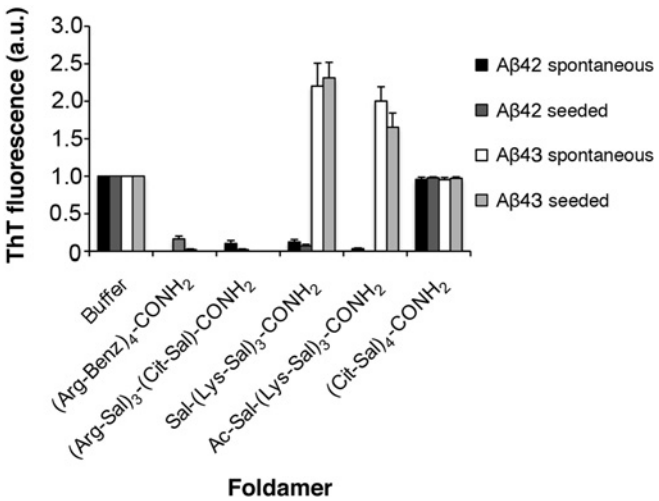

Figure 9 Foldamers inhibit Aβ42 and Aβ43 fibrillization under different assembly conditions

Aβ42 or Aβ43 (5 μM) were incubated with agitation for 16 h at 25 °C without or with Aβ42 fibril seed or Aβ43 fibril seed (0.1 μM monomer) plus or minus 20 μM (Arg-Benz)$_4$-CONH$_2$, (Arg-Sal)$_3$-(Cit-Sal)-CONH$_2$, Sal-(Lys-Sal)$_3$-CONH$_2$, Ac-Sal-(Lys-Sal)$_3$-CONH$_2$ or (Cit-Sal)$_4$-CONH$_2$. Fibrillization was assessed by ThT fluorescence. Values represent means $\pm$ S.E.M. ($n = 3$).

Aβ42 and Aβ43 conformers (Figure 10A). (Arg-Benz)$_4$-CONH$_2$, Sal-(Lys-Sal)$_3$-CONH$_2$ and Ac-Sal-(Lys-Sal)$_3$-CONH$_2$ had no effect on the abundance of A11-reactive Aβ42 or Aβ43 oligomers after 0.5 h (Figure 10A, grey bars). Thus, these foldamers inhibit spontaneous Aβ42 or Aβ43 fibrillization without affecting the formation of A11-reactive conformers. Furthermore, after 4 h in the presence of (Arg-Benz)$_4$-CONH$_2$, Sal-(Lys-Sal)$_3$-CONH$_2$ and Ac-Sal-(Lys-Sal)$_3$-CONH$_2$, A11-reactive Aβ42 species remained at higher levels and did not decline as much as they did in the absence of foldamer (Figure 10A, white bars). Thus, (Arg-Benz)$_4$-CONH$_2$, Sal-(Lys-Sal)$_3$-CONH$_2$, and Ac-Sal-(Lys-Sal)$_3$-CONH$_2$ stabilize A11-reactive conformers. (Arg-Benz)$_4$-CONH$_2$, but not Sal-(Lys-Sal)$_3$-CONH$_2$ or Ac-Sal-(Lys-Sal)$_3$-CONH$_2$, had a similar effect on A11-reactive Aβ43 species (Figure 10A). By contrast, A11-reactive Aβ43 species declined more extensively after 4 h in the presence of Sal-(Lys-Sal)$_3$-CONH$_2$ or Ac-Sal-(Lys-Sal)$_3$-CONH$_2$ (Figure 10A, white bars), which do not inhibit spontaneous Aβ43 fibrillization (Figures 7C and 7D).

(Arg-Sal)$_3$-(Cit-Sal)-CONH$_2$ inhibited the formation of A11-reactive Aβ42 and Aβ43 conformers after 0.5 h (Figure 10A, grey bars). After 4 h, (Arg-Sal)$_3$-(Cit-Sal)-CONH$_2$ prevented further accumulation of A11-reactive Aβ42 and Aβ43 conformers (Figure 10A, white bars). Thus, (Arg-Sal)$_3$-(Cit-Sal)-CONH$_2$ inhibits fibrillization as well as toxic oligomer formation by Aβ42 and Aβ43. (Arg-Sal)$_3$-(Cit-Sal)-CONH$_2$ might inhibit Aβ42 and Aβ43 misfolding by a mechanism that is distinct to the other foldamers and arrests Aβ42 and Aβ43 misfolding prior to an A11-reactive oligomeric state.

(Arg-Sal)$_3$-(Cit-Sal)-CONH$_2$ inhibits formation of toxic Aβ42 and Aβ43 conformers

Next, we evaluated the relative toxicity of Aβ42 and Aβ43 conformers formed in the absence or presence of foldamers. We applied Aβ42 and Aβ43 conformers to SH-SY5Y neuroblastoma cells and assessed cell viability using MTT reduction and LDH release. Foldamers and buffer display little toxicity in the absence

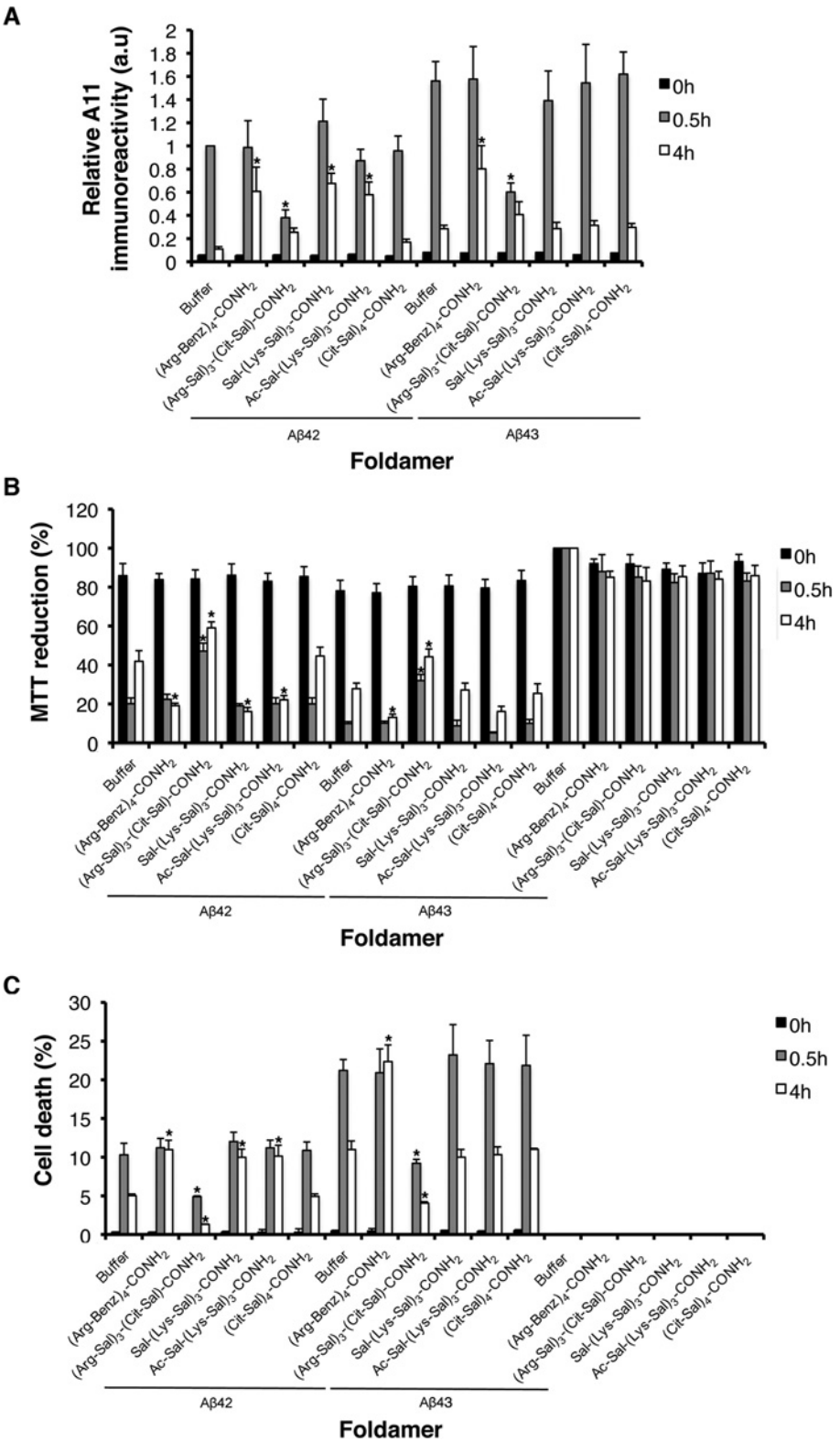

Figure 10 $(Arg\text{-}Sal)_3\text{-}(Cit\text{-}Sal)\text{-}CONH_2$ inhibits formation of toxic Aβ42 and Aβ43 conformers

(**A**–**C**) Aβ42 or Aβ43 (5 μM) was incubated at 25 °C with agitation for 0 h (black bars), 0.5 h (grey bars) or 4 h (white bars) in the absence or presence of 20 μM $(Arg\text{-}Benz)_4\text{-}CONH_2$, $(Arg\text{-}Sal)_3\text{-}(Cit\text{-}Sal)\text{-}CONH_2$, $Sal\text{-}(Lys\text{-}Sal)_3\text{-}CONH_2$, $Ac\text{-}Sal\text{-}(Lys\text{-}Sal)_3\text{-}CONH_2$ or $(Cit\text{-}Sal)_4\text{-}CONH_2$. At the indicated times, the amount of A11-reactive species present (**A**) or toxicity to SH-SY5Y neuroblastoma cells in culture was determined via MTT reduction (**B**) or LDH release (**C**). We also assessed the toxicity of buffer, $(Arg\text{-}Benz)_4\text{-}CONH_2$, $(Arg\text{-}Sal)_3\text{-}(Cit\text{-}Sal)\text{-}CONH_2$, $Sal\text{-}(Lys\text{-}Sal)_3\text{-}CONH_2$, $Ac\text{-}Sal\text{-}(Lys\text{-}Sal)_3\text{-}CONH_2$ or $(Cit\text{-}Sal)_4\text{-}CONH_2$ alone (**B** and **C**). Values represent means ± S.E.M. ($n = 3$). A one-way ANOVA with the post-hoc Dunnett's multiple comparisons test was used to compare Aβ42 plus buffer to each Aβ42 plus foldamer condition (* denotes $P < 0.05$). Likewise, a one-way ANOVA with the post-hoc Dunnett's multiple comparisons test was used to compare Aβ43 plus buffer to each Aβ43 plus foldamer condition (* denotes $P < 0.05$).

of Aβ (Figures 10B and 10C, far right). In the absence of foldamer, Aβ42 and Aβ43 exhibited little toxicity after 0 h (Figures 10B and 10C), consistent with reduced A11 immunoreactivity at this time (Figure 10A). Aβ42 and Aβ43 were more toxic after 0.5 h of assembly than after 4 h (Figures 10B and 10C), indicating that conformers that accumulate at the end of lag phase are more toxic than mature fibrils. In the absence of foldamer, Aβ43 conformers were generally more toxic than Aβ42 conformers (Figures 10B and 10C). The negative control foldamer, $(Cit\text{-}Sal)_4\text{-}CONH_2$, had no effect on toxicity (Figures 10B and 10C). $(Arg\text{-}Benz)_4\text{-}CONH_2$, $Sal\text{-}(Lys\text{-}Sal)_3\text{-}CONH_2$ and $Ac\text{-}Sal\text{-}(Lys\text{-}Sal)_3\text{-}CONH_2$ had no effect on the toxicity of Aβ42 conformers after 0.5 h of assembly (Figures 10B and 10C, grey bars), but after 4 h of assembly the toxicity of Aβ42 conformers was enhanced (Figures 10B and 10C, white bars). Thus, $(Arg\text{-}Benz)_4\text{-}CONH_2$, $Sal\text{-}(Lys\text{-}Sal)_3\text{-}CONH_2$ and $Ac\text{-}Sal\text{-}(Lys\text{-}Sal)_3\text{-}CONH_2$ inhibit spontaneous Aβ42 fibrillization such that more toxic conformers are maintained (Figures 10A–C). For Aβ43, neither $Sal\text{-}(Lys\text{-}Sal)_3\text{-}CONH_2$ nor $Ac\text{-}Sal\text{-}(Lys\text{-}Sal)_3\text{-}CONH_2$ affected the toxicity of conformers after 0.5 h or 4 h (Figures 10B and 10C). However, as for Aβ42, $(Arg\text{-}Benz)_4\text{-}CONH_2$ had no effect on the toxicity of Aβ43 conformers after 0.5 h of assembly (Figures 10B and 10C, grey bars), but after 4 h the toxicity of Aβ43 conformers was enhanced (Figures 10B and 10C, white bars). Thus, $(Arg\text{-}Benz)_4\text{-}CONH_2$ inhibits spontaneous Aβ43 fibrillization in a manner that maintains toxic conformers (Figures 10A–10C).

$(Arg\text{-}Sal)_3\text{-}(Cit\text{-}Sal)\text{-}CONH_2$, which inhibited the formation of A11-reactive Aβ42 and Aβ43 conformers after 0.5 h (Figure 10A, grey bars), also partially reduced the toxicity of Aβ42 and Aβ43 conformers at this time (Figures 10B and 10C, grey bars) and at 4 h (Figures 10B and 10C, white bars). Although Aβ42 and Aβ43 conformers still conferred toxicity in comparison with buffer controls, $(Arg\text{-}Sal)_3\text{-}(Cit\text{-}Sal)\text{-}CONH_2$ was the only foldamer that antagonized Aβ42 and Aβ43 toxicity.

$(Arg\text{-}Sal)_3\text{-}(Cit\text{-}Sal)\text{-}CONH_2$ inhibits spontaneous and seeded Aβ42 and Aβ43 fibrillization and reduces accumulation of toxic Aβ42 and Aβ43 conformers. This combination of properties could have therapeutic potential for three reasons. First, $(Arg\text{-}Sal)_3\text{-}(Cit\text{-}Sal)\text{-}CONH_2$ antagonizes Aβ42 as well as Aβ43, which is an often overlooked but highly toxic Aβ species [13–16]. Secondly, $(Arg\text{-}Sal)_3\text{-}(Cit\text{-}Sal)\text{-}CONH_2$ inhibits the formation of toxic Aβ42 and Aβ43 conformers, which could reduce localized neurodegeneration [65]. Thirdly, $(Arg\text{-}Sal)_3\text{-}(Cit\text{-}Sal)\text{-}CONH_2$ inhibits seeded Aβ42 and Aβ43 assembly, which could prevent the spreading of Aβ pathology throughout the brain in AD [29–31]. Further studies are needed to assess the utility of $(Arg\text{-}Sal)_3\text{-}(Cit\text{-}Sal)\text{-}CONH_2$ against Aβ misfolding and toxicity in the metazoan nervous system.

Future studies will reveal the mechanisms by which foldamers antagonize Aβ-misfolding. Foldamers have amides oriented appropriately (Figure 2) to block growth from fibril ends during seeded polymerization. They are also relatively flat and aromatic (Figure 2) and might antagonize secondary nucleation by binding to the lateral surface of fibrils. Foldamer insertion into molten oligomers could inhibit rearrangement events required for nucleation during spontaneous assembly. Differences in the ability of specific foldamers to inhibit Aβ42 fibrillization compared with Aβ43 fibrillization probably reflect differential antagonism of events driven by the additional C-terminal steric zipper hexapeptide ($G^{38}VVIAT^{43}$) of Aβ43.

Aromatic foldamers could be useful amyloidogenesis inhibitors for various disease-associated proteins. Indeed, another class of aromatic foldamer inhibits amylin fibrillization, which is connected to Type 2 diabetes [66]. Thus, foldamers await further development to antagonize protein misfolding in several settings.

AUTHOR CONTRIBUTION

Conceived and designed the experiments: Katelyn Seither, Heather McMahon, Nikita Singh, Hejia Wang, Mimi Cushman-Nick, Geronda Montalvo, William DeGrado and James Shorter. Performed the experiments: Katelyn Seither, Heather McMahon, Nikita Singh, Hejia Wang, Mimi Cushman-Nick and James Shorter. Analysed the data: Katelyn Seither, Heather McMahon, Nikita Singh, Hejia Wang, Mimi Cushman-Nick, Geronda Montalvo, William DeGrado and James Shorter. Contributed key reagents/materials: Geronda Montalvo and William DeGrado. Wrote the paper: Katelyn Seither, William DeGrado and James Shorter.

FUNDING

This work was supported by the National Institutes of Health [grant numbers T32AG000255 and F31NS067890 (to M.C.N.), GM54616 (to W.F.D.), DP2OD002177 (to J.S.), R21NS067354 (to J.S.), R21HD074510 (to J.S.) and R01GM099836 (to J.S.)]; National Science Foundation Materials Research Science and Engineering Centers grant to the Laboratory for Research on the Structure of Matter of the University of Pennsylvania [grant number DMR-1120901 (to W.F.D.)]; Muscular Dystrophy Association Research Award [grant number MDA277268]; Packard Center for ALS Research at Johns Hopkins University, Target ALS and an Ellison Medical Foundation New Scholar in Aging Award (to J.S.)].

REFERENCES

1 Cushman, M., Johnson, B. S., King, O. D., Gitler, A. D. and Shorter, J. (2010) Prion-like disorders: blurring the divide between transmissibility and infectivity. J. Cell Sci. **123**, 1191–1201 CrossRef PubMed

2 Eisenberg, D. and Jucker, M. (2012) The amyloid state of proteins in human diseases. Cell **148**, 1188–1203 CrossRef PubMed

3 Bieschke, J., Herbst, M., Wiglenda, T., Friedrich, R. P., Boeddrich, A., Schiele, F., Kleckers, D., Lopez del Amo, J. M., Grüning, B. A., Wang, Q. et al. (2012) Small-molecule conversion of toxic oligomers to nontoxic β-sheet-rich amyloid fibrils. Nat. Chem. Biol. **8**, 93–101 CrossRef

4 Wang, H., Duennwald, M. L., Roberts, B. E., Rozeboom, L. M., Zhang, Y. L., Steele, A. D., Krishnan, R., Su, L. J., Griffin, D., Mukhopadhyay, S. et al. (2008) Direct and selective elimination of specific prions and amyloids by 4,5-dianilinophthalimide and analogs. Proc. Natl. Acad. Sci. U.S.A. **105**, 7159–7164 CrossRef PubMed

5 Ehrnhoefer, D. E., Bieschke, J., Boeddrich, A., Herbst, M., Masino, L., Lurz, R., Engemann, S., Pastore, A. and Wanker, E. E. (2008) EGCG redirects amyloidogenic polypeptides into unstructured, off-pathway oligomers. Nat. Struct. Mol. Biol. **15**, 558–566 CrossRef PubMed

6 Blanchard, B. J., Chen, A., Rozeboom, L. M., Stafford, K. A., Weigele, P. and Ingram, V. M. (2004) Efficient reversal of Alzheimer's disease fibril formation and elimination of neurotoxicity by a small molecule. Proc. Natl. Acad. Sci. U.S.A. **101**, 14326–14332 CrossRef PubMed

7 Roberts, B. E. and Shorter, J. (2008) Escaping amyloid fate. Nat. Struct. Mol. Biol. **15**, 544–546 CrossRef PubMed

8 Bulawa, C. E., Connelly, S., Devit, M., Wang, L., Weigel, C., Fleming, J. A., Packman, J., Powers, E. T., Wiseman, R. L., Foss, T. R. et al. (2012) Tafamidis, a potent and selective transthyretin kinetic stabilizer that inhibits the amyloid cascade. Proc. Natl. Acad. Sci. U.S.A. **109**, 9629–9634 CrossRef PubMed

9 Nencetti, S., Rossello, A. and Orlandini, E. (2013) Tafamidis (Vyndaqel): a light for FAP patients. ChemMedChem **8**, 1617–1619

10 Dasilva, K. A., Shaw, J. E. and McLaurin, J. (2010) Amyloid-beta fibrillogenesis: structural insight and therapeutic intervention. Exp. Neurol. **223**, 311–321 CrossRef PubMed

11 Goedert, M. and Spillantini, M. G. (2006) A century of Alzheimer's disease. Science **314**, 777–781 CrossRef PubMed

12 Holtzman, D. M., Morris, J. C. and Goate, A. M. (2011) Alzheimer's disease: the challenge of the second century. Sci. Transl. Med. **3**, 77sr71

13 Saito, T., Suemoto, T., Brouwers, N., Sleegers, K., Funamoto, S., Mihira, N., Matsuba, Y., Yamada, K., Nilsson, P., Takano, J. et al. (2011) Potent amyloidogenicity and pathogenicity of Aβ43. Nat. Neurosci. **14**, 1023–1032 CrossRef PubMed

14 Zou, K., Liu, J., Watanabe, A., Hiraga, S., Liu, S., Tanabe, C., Maeda, T., Terayama, Y., Takahashi, S., Michikawa, M. and Komano, H. (2013) Aβ43 is the earliest-depositing Aβ species in APP transgenic mouse brain and is converted to Aβ41 by two active domains of ACE. Am. J. Pathol. **182**, 2322–2331 CrossRef PubMed

15 Sandebring, A., Welander, H., Winblad, B., Graff, C. and Tjernberg, L. O. (2013) The pathogenic Aβ43 is enriched in familial and sporadic Alzheimer disease. PLoS ONE **8**, e55847 CrossRef PubMed

16 Welander, H., Frånberg, J., Graff, C., Sundström, E., Winblad, B. and Tjernberg, L. O. (2009) Abeta43 is more frequent than Abeta40 in amyloid plaque cores from Alzheimer disease brains. J. Neurochem. **110**, 697–706 CrossRef PubMed

17 Yan, Y. and Wang, C. (2007) Abeta40 protects non-toxic Abeta42 monomer from aggregation. J. Mol. Biol. **369**, 909–916 CrossRef PubMed

18 Kim, J., Onstead, L., Randle, S., Price, R., Smithson, L., Zwizinski, C., Dickson, D. W., Golde, T. and McGowan, E. (2007) Abeta40 inhibits amyloid deposition *in vivo*. J. Neurosci. **27**, 627–633 CrossRef PubMed

19 Colletier, J. P., Laganowsky, A., Landau, M., Zhao, M., Soriaga, A. B., Goldschmidt, L., Flot, D., Cascio, D., Sawaya, M. R. and Eisenberg, D. (2011) Molecular basis for amyloid-β polymorphism. Proc. Natl. Acad. Sci. U.S.A. **108**, 16938–16943 CrossRef PubMed

20 Jarrett, J. T., Berger, E. P. and Lansbury, Jr, P. T. (1993) The carboxy terminus of the beta amyloid protein is critical for the seeding of amyloid formation: implications for the pathogenesis of Alzheimer's disease. Biochemistry **32**, 4693–4697 CrossRef PubMed

21 Kayed, R., Head, E., Thompson, J. L., McIntire, T. M., Milton, S. C., Cotman, C. W. and Glabe, C. G. (2003) Common structure of soluble amyloid oligomers implies common mechanism of pathogenesis. Science **300**, 486–489 CrossRef PubMed

22 Lee, J., Culyba, E. K., Powers, E. T. and Kelly, J. W. (2011) Amyloid-β forms fibrils by nucleated conformational conversion of oligomers. Nat. Chem. Biol. **7**, 602–609 CrossRef PubMed

23 Harper, J. D., Wong, S. S., Lieber, C. M. and Lansbury, P. T. (1997) Observation of metastable Abeta amyloid protofibrils by atomic force microscopy. Chem. Biol. **4**, 119–125 CrossRef PubMed

24 Ladiwala, A. R., Litt, J., Kane, R. S., Aucoin, D. S., Smith, S. O., Ranjan, S., Davis, J., Van Nostrand, W. E. and Tessier, P. M. (2012) Conformational differences between two amyloid beta oligomers of similar size and dissimilar toxicity. J. Biol. Chem. **287**, 24765–24773 CrossRef PubMed

25 Stroud, J. C., Liu, C., Teng, P. K. and Eisenberg, D. (2012) Toxic fibrillar oligomers of amyloid-β have cross-β structure. Proc. Natl. Acad. Sci. U.S.A. **109**, 7717–7722 CrossRef PubMed

26 Lesné, S., Koh, M. T., Kotilinek, L., Kayed, R., Glabe, C. G., Yang, A., Gallagher, M. and Ashe, K. H. (2006) A specific amyloid-beta protein assembly in the brain impairs memory. Nature **440**, 352–357 CrossRef PubMed

27 Bitan, G., Lomakin, A. and Teplow, D. B. (2001) Amyloid beta-protein oligomerization: prenucleation interactions revealed by photo-induced cross-linking of unmodified proteins. J. Biol. Chem. **276**, 35176–35184 CrossRef PubMed

28 Harper, J. D., Lieber, C. M. and Lansbury, Jr, P. T. (1997) Atomic force microscopic imaging of seeded fibril formation and fibril branching by the Alzheimer's disease amyloid-beta protein. Chem. Biol. **4**, 951–959 CrossRef PubMed

29 Jucker, M. and Walker, L. C. (2013) Self-propagation of pathogenic protein aggregates in neurodegenerative diseases. Nature **501**, 45–51 CrossRef PubMed

30 Eisele, Y. S., Obermüller, U., Heilbronner, G., Baumann, F., Kaeser, S. A., Wolburg, H., Walker, L. C., Staufenbiel, M., Heikenwalder, M. and Jucker, M. (2010) Peripherally applied Abeta-containing inoculates induce cerebral beta-amyloidosis. Science **330**, 980–982 CrossRef PubMed

31 Meyer-Luehmann, M., Coomaraswamy, J., Bolmont, T., Kaeser, S., Schaefer, C., Kilger, E., Neuenschwander, A., Abramowski, D., Frey, P., Jaton, A. L. et al. (2006) Exogenous induction of cerebral beta-amyloidogenesis is governed by agent and host. Science **313**, 1781–1784 CrossRef PubMed

32 Cohen, S. I., Linse, S., Luheshi, L. M., Hellstrand, E., White, D. A., Rajah, L., Otzen, D. E., Vendruscolo, M., Dobson, C. M. and Knowles, T. P. (2013) Proliferation of amyloid-β42 aggregates occurs through a secondary nucleation mechanism. Proc. Natl. Acad. Sci. U.S.A. **110**, 9758–9763 CrossRef PubMed

33 Cohen, S. I., Vendruscolo, M., Dobson, C. M. and Knowles, T. P. (2012) From macroscopic measurements to microscopic mechanisms of protein aggregation. J. Mol. Biol. **421**, 160–171 CrossRef PubMed

34 Meisl, G., Yang, X., Hellstrand, E., Frohm, B., Kirkegaard, J. B., Cohen, S. I., Dobson, C. M., Linse, S. and Knowles, T. P. (2014) Differences in nucleation behavior underlie the contrasting aggregation kinetics of the Aβ40 and Aβ42 peptides. Proc. Natl. Acad. Sci. U.S.A. **111**, 9384–9389 CrossRef PubMed

35 Lu, J. X., Qiang, W., Yau, W. M., Schwieters, C. D., Meredith, S. C. and Tycko, R. (2013) Molecular structure of beta-amyloid fibrils in Alzheimer's disease brain tissue. Cell **154**, 1257–1268 CrossRef PubMed

36 Petkova, A. T., Leapman, R. D., Guo, Z., Yau, W. M., Mattson, M. P. and Tycko, R. (2005) Self-propagating, molecular-level polymorphism in Alzheimer's beta-amyloid fibrils. Science **307**, 262–265 CrossRef PubMed

37 Aguzzi, A. and Gitler, A. D. (2013) A template for new drugs against Alzheimer's disease. Cell **154**, 1182–1184 CrossRef PubMed

38 Stöhr, J., Condello, C., Watts, J. C., Bloch, L., Oehler, A., Nick, M., DeArmond, S. J., Giles, K., DeGrado, W. F. and Prusiner, S. B. (2014) Distinct synthetic Aβ prion strains producing different amyloid deposits in bigenic mice. Proc. Natl. Acad. Sci. U.S.A. **111**, 10329–10334 CrossRef PubMed

39 Ladiwala, A. R., Dordick, J. S. and Tessier, P. M. (2011) Aromatic small molecules remodel toxic soluble oligomers of amyloid beta through three independent pathways. J. Biol. Chem. **286**, 3209–3218 CrossRef PubMed

40 Findeis, M. A., Musso, G. M., Arico-Muendel, C. C., Benjamin, H. W., Hundal, A. M., Lee, J. J., Chin, J., Kelley, M., Wakefield, J., Hayward, N. J. and Molineaux, S. M. (1999) Modified-peptide inhibitors of amyloid beta-peptide polymerization. Biochemistry **38**, 6791–6800 CrossRef PubMed

41 McKoy, A. F., Chen, J., Schupbach, T. and Hecht, M. H. (2012) A novel inhibitor of amyloid β (Aβ) peptide aggregation: from high throughput screening to efficacy in an animal model of Alzheimer disease. J. Biol. Chem. **287**, 38992–39000 CrossRef PubMed

42 Cheng, P. N., Liu, C., Zhao, M., Eisenberg, D. and Nowick, J. S. (2012) Amyloid β-sheet mimics that antagonize protein aggregation and reduce amyloid toxicity. Nat. Chem. **4**, 927–933 CrossRef PubMed

43 Evans, C. G., Wisen, S. and Gestwicki, J. E. (2006) Heat shock proteins 70 and 90 inhibit early stages of amyloid beta-(1–42) aggregation *in vitro*. J. Biol. Chem. **281**, 33182–33191 CrossRef PubMed

44 Ladiwala, A. R., Bhattacharya, M., Perchiacca, J. M., Cao, P., Raleigh, D. P., Abedini, A., Schmidt, A. M., Varkey, J., Langen, R. and Tessier, P. M. (2012) Rational design of potent domain antibody inhibitors of amyloid fibril assembly. Proc. Natl. Acad. Sci. U.S.A. **109**, 19965–19970 CrossRef PubMed

45 DeSantis, M. E., Leung, E. H., Sweeny, E. A., Jackrel, M. E., Cushman-Nick, M., Neuhaus-Follini, A., Vashist, S., Sochor, M. A., Knight, M. N. and Shorter, J. (2012) Operational plasticity enables Hsp104 to disaggregate diverse amyloid and nonamyloid clients. Cell **151**, 778–793 CrossRef PubMed

46 Gellman, S. H. (1998) Foldamers: a manifesto. Acc. Chem. Res. **31**, 173–180 CrossRef

47 Mensa, B., Kim, Y. H., Choi, S., Scott, R., Caputo, G. A. and DeGrado, W. F. (2011) Antibacterial mechanism of action of arylamide foldamers. Antimicrob. Agents Chemother. **55**, 5043–5053 CrossRef PubMed

48 Tew, G. N., Scott, R. W., Klein, M. L. and Degrado, W. F. (2010) *De novo* design of antimicrobial polymers, foldamers, and small molecules: from discovery to practical applications. Acc. Chem. Res. **43**, 30–39 CrossRef PubMed

49 Choi, S., Clements, D. J., Pophristic, V., Ivanov, I., Vemparala, S., Bennett, J. S., Klein, M. L., Winkler, J. D. and DeGrado, W. F. (2005) The design and evaluation of heparin-binding foldamers. Angew. Chem. Int. Ed. Engl. **44**, 6685–6689 CrossRef PubMed

50 Goodman, C. M., Choi, S., Shandler, S. and DeGrado, W. F. (2007) Foldamers as versatile frameworks for the design and evolution of function. Nat. Chem. Biol. **3**, 252–262 CrossRef PubMed

51 Liu, C., Zhao, M., Jiang, L., Cheng, P. N., Park, J., Sawaya, M. R., Pensalfini, A., Gou, D., Berk, A. J., Glabe, C. G., Nowick, J. and Eisenberg, D. (2012) Out-of-register β-sheets suggest a pathway to toxic amyloid aggregates. Proc. Natl. Acad. Sci. U.S.A. **109**, 20913–20918 CrossRef PubMed

52 Zheng, J., Liu, C., Sawaya, M. R., Vadla, B., Khan, S., Woods, R. J., Eisenberg, D., Goux, W. J. and Nowick, J. S. (2011) Macrocyclic beta-sheet peptides that inhibit the aggregation of a tau-protein-derived hexapeptide. J. Am. Chem. Soc. **133**, 3144–3157 CrossRef PubMed

53 Kang, S. W., Gothard, C. M., Maitra, S., Wahab, A. T. and Nowick, J. S. (2007) A new class of macrocyclic receptors from iota-peptides. J. Am. Chem. Soc. **129**, 1486–1487 CrossRef PubMed

54 Guichard, G. and Huc, I. (2011) Synthetic foldamers. Chem. Commun. **47**, 5933–5941 CrossRef PubMed

55 Montalvo, G. L., Zhang, Y., Young, T. M., Costanzo, M. J., Freeman, K. B., Wang, J., Clements, D. J., Magavern, E., Kavash, R. W., Scott, R. W. et al. (2014) *De novo* design of self-assembling foldamers that inhibit heparin-protein interactions. ACS Chem. Biol. **9**, 967–975 CrossRef PubMed

56 Rahimi, F., Maiti, P. and Bitan, G. (2009) Photo-induced cross-linking of unmodified proteins (PICUP) applied to amyloidogenic peptides. J. Vis. Exp. **2009**, 1071 doi: 10.3791/1071 CrossRef PubMed

57 Roberts, B. E., Duennwald, M. L., Wang, H., Chung, C., Lopreiato, N. P., Sweeny, E. A., Knight, M. N. and Shorter, J. (2009) A synergistic small-molecule combination directly eradicates diverse prion strain structures. Nat. Chem. Biol. **5**, 936–946 CrossRef PubMed

58 Sun, Z., Diaz, Z., Fang, X., Hart, M. P., Chesi, A., Shorter, J. and Gitler, A. D. (2011) Molecular determinants and genetic modifiers of aggregation and toxicity for the ALS disease protein FUS/TLS. PLoS Biol. **9**, e1000614 CrossRef PubMed

59 Gazit, E. (2002) A possible role for pi-stacking in the self-assembly of amyloid fibrils. FASEB J. **16**, 77–83 CrossRef PubMed

60 Bieschke, J., Russ, J., Friedrich, R. P., Ehrnhoefer, D. E., Wobst, H., Neugebauer, K. and Wanker, E. E. (2010) EGCG remodels mature alpha-synuclein and amyloid-beta fibrils and reduces cellular toxicity. Proc. Natl. Acad. Sci. U.S.A. **107**, 7710–7715 CrossRef PubMed

61 Porat, Y., Abramowitz, A. and Gazit, E. (2006) Inhibition of amyloid fibril formation by polyphenols: structural similarity and aromatic interactions as a common inhibition mechanism. Chem. Biol. Drug Des. **67**, 27–37 CrossRef PubMed
62 Das, U., Hariprasad, G., Ethayathulla, A. S., Manral, P., Das, T. K., Pasha, S., Mann, A., Ganguli, M., Verma, A. K., Bhat, R. et al. (2007) Inhibition of protein aggregation: supramolecular assemblies of arginine hold the key. PLoS One. **2**, e1176 CrossRef PubMed
63 Shorter, J. (2010) Emergence and natural selection of drug-resistant prions. Mol. Biosyst. **6**, 1115–1130 CrossRef PubMed
64 King, O. D., Gitler, A. D. and Shorter, J. (2012) The tip of the iceberg: RNA-binding proteins with prion-like domains in neurodegenerative disease. Brain Res. **1462**, 61–80 CrossRef PubMed
65 Meyer-Luehmann, M., Spires-Jones, T. L., Prada, C., Garcia-Alloza, M., de Calignon, A., Rozkalne, A., Koenigsknecht-Talboo, J., Holtzman, D. M., Bacskai, B. J. and Hyman, B. T. (2008) Rapid appearance and local toxicity of amyloid-beta plaques in a mouse model of Alzheimer's disease. Nature **451**, 720–724 CrossRef PubMed
66 Kumar, S., Brown, M. A., Nath, A. and Miranker, A. D. (2014) Folded small molecule manipulation of islet amyloid polypeptide. Chem. Biol. **21**, 775–781 CrossRef PubMed

Received 6 December 2013/20 August 2014; accepted 21 August 2014
Published as BJ Immediate Publication 21 August 2014, doi:10.1042/BJ20131609